Transit Time Isolation of a High Power Microwave Amplifier

E. Kuang, T. J. Davis, G. Kerslick, J. A. Nation, and L. Schächter
Laboratory of Plasma Studies and School of Electrical Engineering,
Cornell University, Ithaca, New York 14853
(Received 2 June 1993)

We report experimental results from a high power X-band traveling wave tube amplifier designed to eliminate sidebands due to reflections from its output. The amplifier has a very low energy velocity, such that the time it takes a wave to be reflected from the output to the input is of the order of, or greater than, the electron beam pulse duration. The bandwidth of the output spectrum is limited by the very narrow passband of the periodic structure. The amplifier has been operated at power levels of up to 160 MW at 9 GHz for pulse durations of 50 ns.

PACS numbers: 85.10.Jz, 41.75.Ht

The high power microwave requirements of the next linear collider (NLC) are very demanding, typically of order 200 MW per meter of acceleration structure. This is expected to correspond to a gradient of 100 MV/m for a pulse duration of more than 100 ns. The general trend in this area of research [1] is to expand beyond the S-band klystron to frequencies in the range 10–35 GHz. The main reason for this trend is that for a given accelerating gradient the necessary microwave power varies qualitatively as the inverse of the operating frequency squared ($P \propto f^{-2}$). Thus an increase by a factor of 3 in the frequency can lower the necessary power by 1 order of magnitude. This increase in the frequency is accompanied by a corresponding reduction in the physical dimensions of the klystron's cavities and drifting region. This becomes a significant drawback when rf breakdown is considered. The smaller the volume of the cavity, for a given stored energy, the larger the electric fields and thus the probability of rf breakdown increases. This problem becomes acute in the extraction cavity.

In order to overcome this problem it is possible to replace the extraction cavity by a traveling wave structure, i.e., a disk loaded waveguide. Unlike the klystron where the cavities are electromagnetically isolated (by the drift region which is below cutoff) the traveling wave structure is a set of coupled cavities. In this case the beam-wave interaction is distributed along the entire interaction length whereas in a klystron it is limited to the close vicinity of the cavity.

The use of traveling wave amplifiers for the production of high power microwave radiation in the X band has been reported previously [2–5]. In a single stage amplifier, which consists of a section of corrugated waveguide, driven by a 0.85 MV, 0.8–1.6 kA, 100 ns electron beam, total power levels of up to 150 MW were measured. Beyond these power levels the system was noisy and prone to oscillation. In addition, for output powers above 80 MW the output spectrum showed the development of sidebands.

The coupling between the cavities also permits a backward electromagnetic wave to propagate. At very high gain this wave may cause the system to oscillate. To avoid the single stage oscillations, which are caused by the reflection of an electromagnetic wave from the output end of the amplifier to its input, a two-stage severed amplifier was developed. This device consists of two rippled wall waveguides isolated from each other by a sever, consisting of a lossy section of waveguide operated below cutoff. The space charge waves, which develop along the beam in the first stage, propagate through the sever whereas the electromagnetic mode is strongly (−25 dB) attenuated. In addition, the sever attenuates the reflected wave from the output end of the second stage, and prevents system oscillation due to feedback. With this device total power levels of up to 400 MW were achieved for beam currents of 0.8–1.2 kA and with an efficiency of more than 40%. Sidebands were observed at all output power levels in the two-stage amplifier, with the output spectrum extending over 300 MHz. The sidebands were asymmetrically located with respect to the input frequency and at the highest output levels carried up to 50% of the power.

In parallel with these experiments, theoretical analysis [6–9] has shown several interesting results: (i) As a result of the interaction process the energy spread of *individual* electrons can be as high as 60% of the initial beam energy, while the *average* energy of the beam is reduced by less than 10% [6]. (ii) When end effects are included the pure electromagnetic transmission characteristics of a slow wave structure are dominated by reflections which cause a frequency dependent standing wave pattern. This results in waves of certain frequencies being preferentially transmitted, whereas others are partially reflected. The separation of the transmission peaks, Δf, is determined by the total length of the structure d and the group velocity ($V_{\rm gr}$) by the relation $\Delta f = V_{\rm gr}/2d$. In the presence of an electron beam the peak value of the transmission coefficient increases due to the gain but the separation of discrete peaks remains unchanged. Consequently, the effective bandwidth of the interaction becomes narrower

0031-9007/93/71(16)/2666(4)$06.00

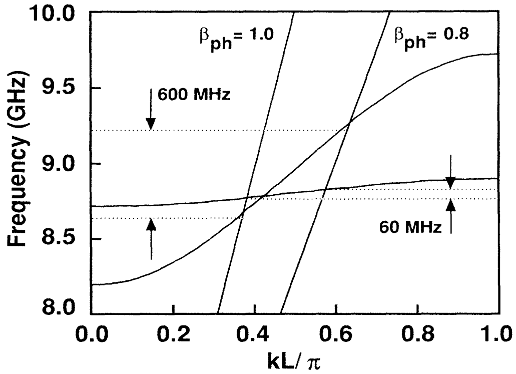

FIG. 1. Dispersion relations for a broad band and for a narrow band periodic structure, illustrating the decrease in bandwidth of an amplified signal in a low group velocity structure.

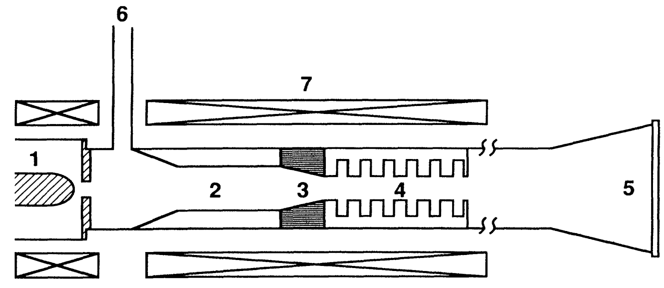

FIG. 2. Schematic showing the assembly of a two-stage severed amplifier. The first stage uses a dielectric loaded amplifier and the second stage a 10 period narrow band (low group velocity) structure. (1) Electron beam diode, (2) dielectric first stage, (3) silicon carbide sever, (4) narrow band structure, (5) output horn, (6) input waveguide, (7) magnetic field coils.

by the gain factor [7]. (iii) The ideal picture of an amplifier is a device in which the wave amplitude grows in space but remains constant in time, whereas in an ideal oscillator the amplitude grows in time but is constant in space. Any practical device operates somewhere between these two limiting cases [8].

Based on these studies we developed a qualitative model which explains the presence of the asymmetric sidebands. The essence of the model is as follows. The electrons are bunched by the wave and, depending on their phase relative to that of the wave, are either accelerated or decelerated. In this process they acquire a broad range of velocities. As they traverse the periodic structure the electrons generate spontaneous radiation in a frequency range which is directly related to their velocity spread: $\delta\omega/\omega \approx \frac{\delta V}{V_0}/(1-V_0/V_{\rm gr})$ where V_0 is the average velocity of the electrons. The electromagnetic output spectrum is determined by the frequency selection due to the reflections and the subsequent amplification of the radiation by the beam. The selected frequencies correspond to the peaks in the transmission coefficient and thus the amplified noise is revealed as asymmetric sidebands, since the transmission peaks are determined primarily by the geometry, and not by the input frequency.

Since an output spectrum wider than 100 MHz is not acceptable for most applications of interest, we designed [9] an amplifier to eliminate the unwanted reflections. In a 15 cm long amplifier with a structure group velocity of $V_{\rm gr} = 0.007c$, it takes about 75 ns for a reflected wave to reach the input. This is approximately equal to the electron pulse duration, and consequently the beam is unaffected by the time the reflected wave amplitude becomes significant at the input to the amplifier. An equivalent interpretation relies on the dispersion relation of two periodic structures; see Fig. 1. If the passband is 1.7 GHz, as in the original amplifier [2,3], an electron velocity spread between $0.8c$ and $1.0c$ can generate noise in a 600 MHz frequency range, whereas in the narrow passband (200 MHz) structure described here, the noise generated restricts the coherent signal to a width of 60 MHz. Transit time isolation in free electron lasers has been used previously to isolate the diagnostics from the input signal [10]. In the remainder of this Letter we report experimental results which show that the transit time isolation design eliminates sideband development.

Figure 2 shows a schematic of the experiment. The first stage is a medium power Cherenkov amplifier [9] which consists of a 1.6 cm radius waveguide partially loaded with STYCAST HIK dielectric material ($\epsilon = 5.0$). It is 30 cm long including a 5 cm taper at the input, and is followed by a 15 cm silicon carbide sever. The narrow band amplifier serves as the second stage of the system and consists of a ten period iris loaded waveguide. The structure has a 1.2 cm period, and a 1.42 cm external radius. Each iris is 0.6 cm long with an internal radius of 0.62 cm. To couple the power out of the narrow band structure, the length of the last iris is reduced to 0.1 cm. This modification is essential for efficient output coupling. The system is driven by a 1 MV, 1 kA, 50 ns, 0.6 cm diam electron beam. The microwave input signal is provided by an X-band magnetron which injects $\sim$ 30 kW into the dielectric first stage. The output power of this single stage alone is of order 3–5 MW, and has been increased to 50 MW before rf breakdown occurs on the dielectric. The main reason for the use of this Cherenkov amplifier was to prebunch the beam, and as a simple method to control reflections from the ends of the first stage.

The output power of the two-stage amplifier is determined using far field measurements of the gain. Figure 3 shows this power as a function of input frequency. Power levels from independent calorimetric measurements [11,12] correlate well with the gain data up to 65 MW. Above this level the pressure transducer in the calorimeter saturated. Output powers of 160 MW at 8.9 GHz have been measured for the full 50 ns electron

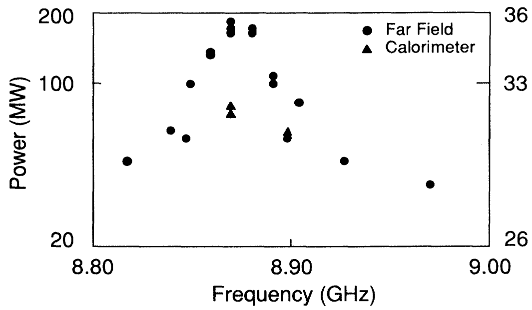

FIG. 3. Measured frequency response of the two-stage amplifier. The triangles indicate calorimetric data and the circles data obtained from the far field measurements. The calorimeter output saturates at about 65 MW.

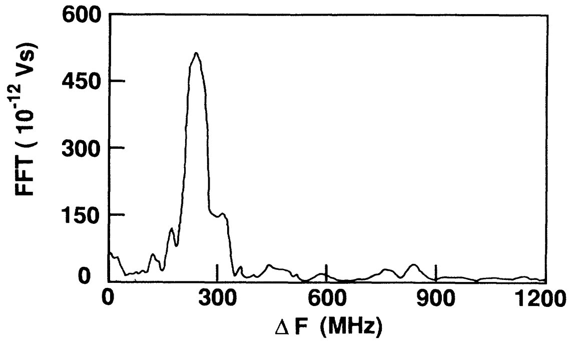

FIG. 4. Fast Fourier transform of the measured output signal from the two-stage amplifier showing the single frequency output.

beam duration. Pulse shortening has been observed at higher power levels of ~180 MW. This may indicate the onset of rf breakdown problems. The frequency content of the sampled output signal is measured with a double balanced mixer using heterodyning techniques. A typical fast Fourier transform (FFT) is illustrated in Fig. 4. The signal is at the input frequency and has a width of 48 MHz. The 50 ns pulse width of the output signal introduces a minimum FFT width of 20 MHz and will produce side lobes in the transform. If we interpret the secondary peaks of the FFT at 9 GHz as sidebands, a worst case scenario, then the sideband level has been reduced by at least 10 dB compared to that achieved in our earlier work [4].

The interaction in the narrow band structure has been studied both analytically and with the particle-in-cell code MAGIC. The analytical results indicate that a gain of 5–7 dB/cm can be expected compared to 1–2 dB/cm in the broad passband structure. This results from the high impedance ($Z \sim 1/V_{gr}$) of such narrow bandwidth amplifiers which, in turn, leads to high values of electric field in the structure. Calculations show that for output powers of 200 MW the electric field on the wall will be 200 MV/m. In order to reduce the interaction impedance and hence the electric stress on the walls a number of options may be available. The design can be modified to maintain the bandwidth, but increase the radius of the iris sections. Alternatively, operation at the first spatial harmonic of the structure may also be considered.

The sever section plays a crucial role in determining the output power level by introducing a change in the phase angle between the current density modulation and the longitudinal E field compared to that in the traveling wave tube section. Our 1D code indicates that the output power may range from 190 MW down to a few MW as the phase shift changes from 300° to 150° at the input to the narrow band structure.

Numerical simulations using the MAGIC code confirm that the sidebands have been essentially eliminated through the use of narrow band structures. The high gain feature within the passband is also confirmed, with the output power level dropping to ~ 6 MW outside the passband. At present we are unable to model the details of the sever within the particle-in-cell code and cannot make a detailed numerical comparison with our experimental results. Further work is in progress to adequately model the sever to include, not only the electromagnetic isolation of the input from the output, but also its influence on the space charge modes.

In conclusion, we have developed a novel technique, transit time isolation, which may be used to eliminate sideband phenomena in high power traveling wave amplifiers. This method may be extended to longer pulse durations than those reported here, but is clearly not appropriate where microsecond pulses may be required. The experimental results are consistent with the main features of analytic and MAGIC code simulations of the amplifier.

This work was supported by the Department of Energy and the Air Force Office of Scientific Research. The MAGIC simulation code was supplied by Mission Research Corporation.

[1] L. Schächter, in Proceedings of the Particle Accelerator Conference, Washington DC, 17–20 May 1993 (to be published).
[2] D. Shiffler, J. A. Nation, and C. B. Wharton, Appl. Phys. Lett. **54**, 674 (1989).
[3] D. Shiffler, J. A. Nation, and G. S. Kerslick, IEEE Trans. Plasma Sci. **18**, 546 (1990).
[4] D. Shiffler, J. A. Nation, J. D. Ivers, G. S. Kerslick, and L. Schächter, J. Appl. Phys. **70**, 106 (1991).
[5] D. Shiffler, J. D. Ivers, G. S. Kerslick, J. A. Nation, and L. Schächter, Appl. Phys. Lett. **58**, 899 (1991).
[6] L. Schächter, J. A. Nation, and G. Kerslick, J. Appl. Phys. **68**, 5874 (1990).
[7] L. Schächter, J. A. Nation, and D. Shiffler, J. Appl. Phys.

70, 114 (1991).
[8] Levi Schächter and J. A. Nation, Phys. Rev. A **45**, 8820 (1992).
[9] Levi Schächter and J. A. Nation, in Proceedings of the Workshop on Advanced Acceleration Concepts, Port Jefferson, June 1992 (to be published).
[10] T. J. Orzechowski, B. Anderson, W. M. Fawley, D. Prosnitz, E. T. Scharlemann, S. Yarema, D. Hopkins, A. C. Paul, A. M. Sessler, and J. Wurtele, Phys. Rev. Lett. **54**, 89 (1985).
[11] E. Garate, H. Kosai, K. Evans, and A. Fisher, Appl. Phys. Lett. **56**, 1092 (1990).
[12] C. B. Wharton, L. M. Earley, and W. P. Ballard, Rev. Sci. Instrum. **57**, 855 (1986).